

# Luminescence in Colorless, Transparent, Thermally Stable Thin Films of $\text{Eu}^{3+}$ and $\text{Tb}^{3+}$ $\beta$ -diketonates in Hybrid Inorganic–Organic Zinc-based Sol–Gel Matrix

Renata Figueredo Martins · Rodrigo Ferreira Silva · Rogéria Rocha Gonçalves · Osvaldo Antonio Serra

Received: 26 November 2008 / Accepted: 7 February 2010 / Published online: 24 February 2010  
© Springer Science+Business Media, LLC 2010

**Abstract** Luminescent zinc-based hybrid inorganic–organic films with rare–earth (RE) complexes have been prepared using a non-alkoxide sol–gel process. The films were fabricated by the dip-coating method starting from zinc acetate dihydrate, rare earth chloride, lactic acid as hydrolytic catalyst, and anhydrous ethanol. The  $\beta$ -diketonates thenoyltrifluoroacetone (Httfa) and dibenzoylmethane (Hdbm) were used as ligands to  $\text{Eu}^{3+}$  and  $\text{Tb}^{3+}$ , respectively. After deposition of the first layer, the films were fired at temperatures between 50 and 300 °C, in air. Photophysical properties such as excitation, emission and emission, lifetimes were determined for the films obtained in different conditions.  $\text{Eu}^{3+}$ /ttfa and  $\text{Tb}^{3+}$ /dbm films fired at 300 and 250 °C, respectively, are still transparent and gave rise to intense emission when excited through the ligand (*antenna* effect).

**Keywords** Luminescence films · Sol–gel process ·  $\beta$ -diketonates · *Antenna* effect · Thermal stability

## Introduction

Lanthanide complexes have been shown to be a class of very promising materials for use as emission devices. This is mainly because the rare earth (RE) luminescence intensity can be improved through ligand-assisted energy transfer, namely the *antenna* effect. The forbidden f-f transitions are enhanced by coordination with appropriate

ligands (light collectors) such as  $\beta$ -diketonates and cripates, where  $\text{Eu}^{3+}$  and  $\text{Tb}^{3+}$  compounds can give emissions with good efficiency in several systems [1]. Another way to enhance the lanthanide emission is to employ embedded inorganic matrices such as the semiconductors GaP [2], ZnO [3],  $\text{TiO}_2$  [4], and sol–gel derived glasses [5]. Among various methodologies, the sol–gel process has been widely employed for preparation of luminescent rare–earth based materials in inorganic hosts in very mild conditions. Most studies have reported hydrolysis and polymerization reactions of the alkoxide precursors using europium and terbium complexes containing coordinated organic ligands ( $\beta$ -diketonates and aromatic carboxylic acids) to prepare powders, bulk monoliths [6–10], and films [11]. However, the use of non-alkoxide precursors is also desirable due to their low cost and non-toxicity [12]. Luminescent films have potential application as organic light-emitting diodes (OLEDs) in large-area flat panels [13–16]. For full-color applications, a set of red, green, and blue emitters with sufficiently high luminous efficiency and proper chromaticity is necessary.

In recent years, zinc oxide films have also become technologically important because of their range of electrical and optical properties, together with their high chemical and mechanical stabilities, which make them suitable for a variety of applications. The preparation of stable colloidal zinc oxide nanoparticles through sol–gel process from non-alkoxide reagents have been well described by Bahnemann et al. [17] and Spanhel et al. [18]. Thin zinc oxide films have been prepared by Tang et al. [19] and Silva et al. [20], through thermal decomposition of a stable precursor colloidal sol prepared from an ethanolic reflux of zinc acetate and lactic acid as the hydrolysis catalyst. A similar procedure has been reported for the preparation of ZnO:Eu films [21]. However, the efficiency of the emission

R. F. Martins · R. F. Silva · R. R. Gonçalves · O. A. Serra (✉)  
Department of Chemistry, FFCLRP-USP,  
Av. dos Bandeirantes, 3900,  
CEP 14040-901 Ribeirão Preto, SP, Brazil  
e-mail: osaserra@usp.br

luminescence of rare earth ions in ZnO matrices is not satisfactory compared with the same ions in other commercialized phosphors. This is due to the large difference in ionic radii between  $\text{Zn}^{2+}$  and the rare earth ions ( $R_{\text{Zn}^{2+}} = 0.06$  nm,  $R_{\text{RE}^{3+}} = 0.10 - 0.12$  nm), which makes penetration of the rare earth ions into the ZnO crystal lattice very difficult [22]. The presence of thermally stable organic ligands capable of acting as an *antenna* and forming an array of strongly absorbing units and a rare earth emitter in an inorganic matrix should produce an efficient light-conversion device. Matrices obtained as described by Tang [19] from non-alkoxide precursors are good candidates to meet such conditions, although no devices have been reported so far.

We describe the fabrication and photophysical properties of colorless, transparent, thermally stable thin films where  $\text{Eu}^{3+}$ /thenoyltrifluoroacetate (tta) and  $\text{Tb}^{3+}$ /dibenzoyl-methanate (dbm) were embedded in a hybrid inorganic–organic zinc-based sol–gel matrix prepared by a non-alkoxide sol–gel process.

## Experimental procedure

The colloidal sols were prepared using methodologies described elsewhere [19, 20]. Ethanolic solutions of the rare earth chlorides ( $0.10$  mol  $\text{L}^{-1}$ ) were added separately to an ethanolic suspension of zinc acetate dihydrate ( $0.44$  mol  $\text{L}^{-1}$ ). The system was kept under reflux, and lactic acid was added until complete dissolution of the solid, thus forming a stable and translucent sol. Solid Htta and Hdbm were added to the sols containing  $\text{Eu}^{3+}$  and  $\text{Tb}^{3+}$ , respectively, and agitated at  $\sim 25$  °C for 30 min. Molar ratios of 1:100 and 1:3 for  $\text{RE}^{3+}/\text{Zn}^{2+}$  and  $\text{RE}^{3+}/\beta$ -diketonate, respectively, were employed. The sols were stable in a closed flask for a long period of time (a month or longer).

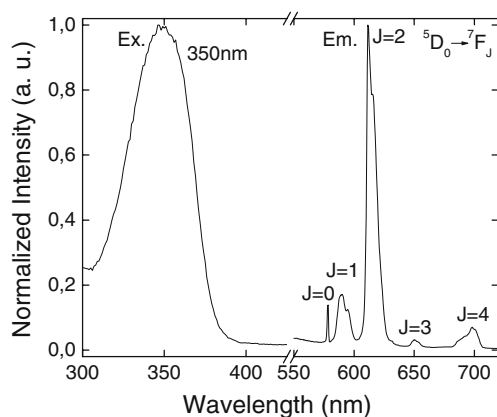


**Fig. 1** Excitation spectrum ( $\lambda_{\text{em}}=612$  nm) and emission spectrum ( $\lambda_{\text{exc}}=350$  nm) of the  $\text{Eu}^{3+}$ /tta film annealed at 150 °C for 15 min

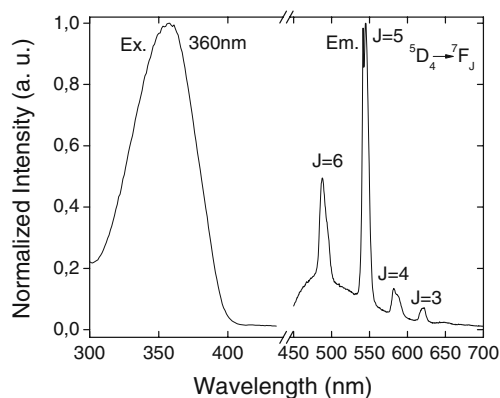


**Fig. 2** Excitation spectrum ( $\lambda_{\text{em}}=543$  nm) and emission spectrum ( $\lambda_{\text{exc}}=360$  nm) of the  $\text{Tb}^{3+}$ /dbm film annealed at 150 °C for 15 min

The films were deposited over borosilicate glass substrates previously washed with a sodium dodecylsulfate detergent, treated ultrasonically with deionized water for 30 min, followed by another 30 min treatment with ethanol, and dried in ambient conditions. As for the transfer process, only one deposition of the 15-day aged sol ( $\sim 25$  °C) onto glass substrates was carried out by dip-coating at  $4.0$  cm  $\text{min}^{-1}$ , and the sol was kept immersed for 30 s. The films were thermally treated at 50, 100, 150, 200, 250, 300, and 350 °C for periods of 15 and 30 min. Thermal stability experiments were performed by heating the films at 150 °C for 15 min, then repeating the procedure until 2 h, and the emission spectrum was obtained after each step.

The emission and excitation spectra of the films were measured using a SPEX TRIAX 550 FLUOROLOG III spectrofluorometer with a 450 W xenon lamp and a Hammamatsu R928 photomultiplier. The luminescence of decay curves were measured using a 1934D phosphorimeter accessory with a pulsed xenon lamp. All measurements were accomplished at room temperature.

## Results and discussion

Figures 1 and 2 show the excitation and emission spectra of the colorless transparent films annealed at 150 °C for 15 min. The excitation spectra of the materials were obtained by monitoring the emission of the  $\text{Eu}^{3+}$  and  $\text{Tb}^{3+}$  ions at 612 nm and 543 nm, respectively. The excitation spectra reveal broad bands with maxima at 350 and 360 nm due to energy transfer from tta and dbm to  $\text{Eu}^{3+}$  and  $\text{Tb}^{3+}$ , respectively. The emission spectrum (Fig. 1) of the  $\text{Eu}^{3+}$ /tta film displays bands at 578, 590, 612, 650, and 698 nm, assigned to the  $^5\text{D}_0 \rightarrow ^7\text{F}_J$  ( $J=0,1,2,3,4$ ) transitions with the hypersensitive  $^5\text{D}_0 \rightarrow ^7\text{F}_2$  red emission as the most prominent group. Figure 2 shows the emission and excitation spectra of the  $\text{Tb}^{3+}$ /dbm film. The emission spectrum

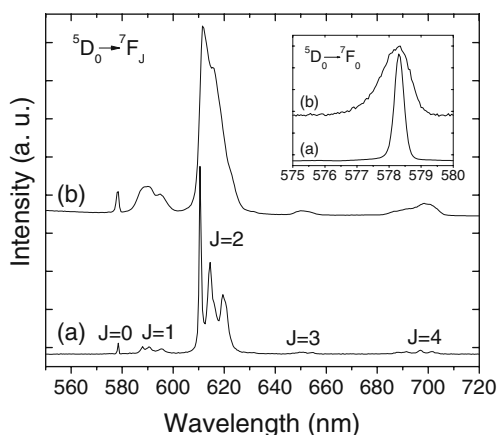


**Fig. 3** Emission spectra of (a)  $\text{Eu}(\text{ttfa})_3 \cdot 2\text{H}_2\text{O}(\text{s})$  and (b)  $\text{Eu}^{3+}/\text{ttfa}$  film annealed at 150 °C for 15 min ( $\lambda_{\text{exc}}=350$  nm)

consists of the typical emission bands of  $\text{Tb}^{3+}$ , at 488, 543, 581, and 622 nm, which are assigned to the  $^5\text{D}_4 \rightarrow ^7\text{F}_J$  ( $J=6,5,4,3$ ) transitions. The strongest  $^5\text{D}_4 \rightarrow ^7\text{F}_5$  green emission is observed at 543 nm. Excitation in the absorption bands of the ligands results in the strong emission of  $\text{Eu}^{3+}$  and  $\text{Tb}^{3+}$ , indicating that an efficient intramolecular energy transfer occurs from the organic ligands to the emitting ions. For the  $\text{Eu}^{3+}/\text{ttfa}$  film, the emission intensity of the forbidden  $^5\text{D}_0 \rightarrow ^7\text{F}_0$  transition (578 nm) is indicative of the absence of an inversion center in the emitting system.

The emission spectra of the  $[\text{Eu}(\text{ttfa})_3 \cdot 2\text{H}_2\text{O}]$  powder (a) and  $\text{Eu}^{3+}/\text{ttfa}$  film (b) excited at 350 nm (Fig. 3) have a similar feature; that is, there is broadening of the bands in the film, as expected for such a system. As shown in the inset, the  $^5\text{D}_0 \rightarrow ^7\text{F}_0$  transition presents a width of  $10 \text{ cm}^{-1}$  at half height for the  $[\text{Eu}(\text{ttfa})_3 \cdot 2\text{H}_2\text{O}]$  powder (a), and  $\sim 35 \text{ cm}^{-1}$  for the  $\text{Eu}^{3+}/\text{ttfa}$  film (b). According to Bünzli et al. [23], when a typical  $^5\text{D}_0 \rightarrow ^7\text{F}_0$  transition presents a sharp component (width  $\sim 2 \text{ cm}^{-1}$  at half height), it reflects

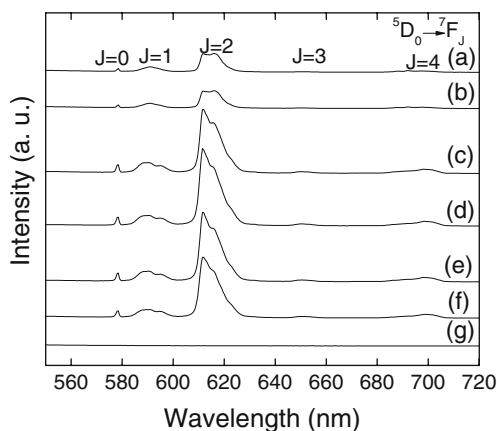


**Fig. 4** Emission spectra ( $\lambda_{\text{exc}}=350$  nm) of the  $\text{Eu}^{3+}/\text{ttfa}$  film annealed at (a) 50 °C, (b) 100 °C, (c) 150 °C, (d) 200 °C, (e) 250 °C, (f) 300 °C, and (g) 350 °C

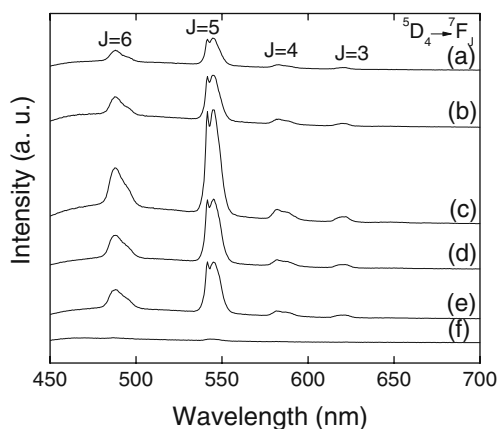


**Fig. 5** Emission spectra ( $\lambda_{\text{exc}}=360$  nm) of the  $\text{Tb}^{3+}/\text{dbm}$  film annealed at (a) 50 °C, (b) 100 °C, (c) 150 °C, (d) 200 °C, (e) 250 °C, and (f) 300 °C

the presence of an only chemical environment for the  $\text{Eu}^{3+}$  ion. A very broad  $^5\text{D}_0 \rightarrow ^7\text{F}_0$  band with a width  $>10 \text{ cm}^{-1}$  at half height suggests that the system has polymeric-like nature or several and very similar environments [24].

In order to study the thermal stability of the films, we investigated the emission intensity as a function of the temperature. Figure 4 presents the emission spectra of the  $\text{Eu}^{3+}/\text{ttfa}$  films heated at 50, 100, 150, 200, 250, 300, and 350 °C for 15 min. The films heated at 150, 200, and 250 °C presented higher emission intensities than those heated at lower temperatures, probably because of the release of water and ethanol from the ion neighborhood, which promote quenching as a result of their high vibrational frequency modes. On the other hand, the films heated at temperatures over 300 °C have a large decrease in the emission intensity, probably because of the ttfa decomposition. A similar behavior is observed for the  $\text{Tb}^{3+}/\text{dbm}$  films (Fig. 5), where the ligand decomposition starts at lower temperatures.

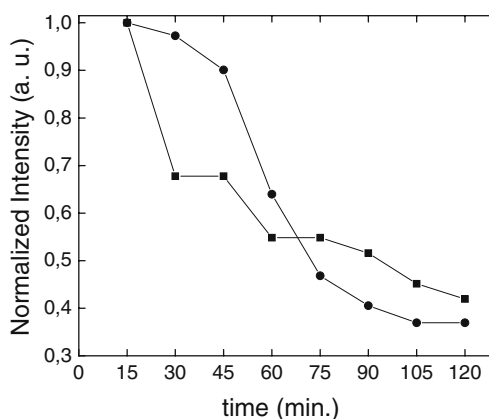


**Fig. 6** Relationship between the emission intensities of the  $^5\text{D}_0 \rightarrow ^7\text{F}_2$  transitions for the (●)  $\text{Eu}^{3+}/\text{ttfa}$  and  $^5\text{D}_4 \rightarrow ^7\text{F}_5$  (■)  $\text{Tb}^{3+}/\text{dbm}$  films heated at 150 °C, and heating time

Emissions ( $^5D_0 \rightarrow ^7F_2$  for  $\text{Eu}^{3+}/\text{tffa}$  and  $^5D_4 \rightarrow ^7F_5$  for  $\text{Tb}^{3+}/\text{dbm}$ ) were measured after the films were heated at 150 °C for 15 min, and this procedure was repeated up to 2 h. The final results are depicted in Fig. 6. The emission intensity of the  $\text{Eu}^{3+}/\text{tffa}$  film decreases more slowly than that of the  $\text{Tb}^{3+}/\text{dbm}$  film, probably because of the lower thermal stability of dbm.

The decay associated with the emissions from the excited states of  $\text{Eu}^{3+}$  ( $^5D_0 \rightarrow ^7F_2$ ) and  $\text{Tb}^{3+}$  ( $^5D_4 \rightarrow ^7F_5$ ) to the respective ground state in the films were analyzed, and it consists of exponential decays. The lifetimes of the  $\text{Eu}^{3+}/\text{tffa}$  films are better fitted through a monoexponential decay, giving an average value of 0.7 ms; for a biexponential decay, the lifetime values were found to be  $\tau_1=0.2$  and  $\tau_2=0.7$  ms. For the  $\text{Tb}^{3+}/\text{dbm}$  films, only a second-order exponential fitting gave better results with average  $\tau_1$  and  $\tau_2$  values of 0.2 and 0.9 ms, respectively. Low emission lifetimes (<0.1 ms) were assigned to radiationless transitions caused by vibrational modes from the surrounding medium and also to amplified stimulated emissions in  $\text{Eu}^{3+}/\beta$ -diketonates under special conditions [25]. Deviations from the determined lifetimes (~0.1 ms) are also in agreement with the broadening of the  $^5D_0 \rightarrow ^7F_0$  transition in the  $\text{Eu}^{3+}/\text{tffa}$  emission spectra, probably due to a multicomponent environment around the ions in the film. A lifetime value of 0.26 ms for  $[\text{Eu}(\text{tffa})_3 \cdot 2\text{H}_2\text{O}]$  is reported in the literature [26, 27], and we found a lifetime of 0.30 ms. As for  $[\text{Tb}(\text{dbm})_3 \cdot 2\text{H}_2\text{O}]$ , a value of 0.60 ms was determined. The lifetimes were calculated by using the Origin<sup>®</sup> graphics software.

Both the  $\text{Eu}(\text{tffa})_3 \cdot 2\text{H}_2\text{O}$  powder and the  $\text{Eu}^{3+}/\text{tffa}$  film show high color purities ( $x = 0.66$  and  $y = 0.34$ ), which is a consequence of the intense bands of the  $^5D_0 \rightarrow ^7F_2$  transitions. For the  $[\text{Tb}(\text{dbm})_3 \cdot 2\text{H}_2\text{O}]$  powder and  $\text{Tb}^{3+}/\text{dbm}$  film, the *Commission Internationale de l'Eclairage* (CIE) color parameters are determined as  $x = 0.23$  and  $y = 0.50$ . The CIE chromaticity coordinates were obtained through the Spectra Lux software [28]. The standard coordinates accepted by the *National Television Standard Committee* (NTSC) for red are  $x = 0.67$  and  $y = 0.33$  [29], and for green the values are  $x = 0.21$  and  $y = 0.71$  [30].

## Conclusions

Luminescent zinc-based hybrid inorganic–organic films with  $\text{Eu}^{3+}$  and  $\text{Tb}^{3+}$  complexes can be successfully prepared from non-alkoxide reagents through a sol–gel process. Such thin films are a very promising transparent luminescent material due to the efficient energy transfer from the ligands tffa and dbm to the  $\text{Eu}^{3+}$  and  $\text{Tb}^{3+}$  ions, respectively, and to their high thermal stability. Furthermore, the current synthesis method can be easily applied to other ligands and luminescent rare earths.

**Acknowledgements** The authors are grateful to the Brazilian research funding agencies Coordenação de Aperfeiçoamento de Pessoal de Nível Superior (CAPES), Conselho Nacional de Desenvolvimento Científico e Tecnológico (CNPq), and Fundação de Amparo à Pesquisa do Estado de São Paulo (FAPESP) for financial support and grants. The authors also gratefully thank Dr. C. M. C. P. Manso for helpful discussions.

## References

- Lehn J-M (1988) Supramolecular chemistry—scope and perspectives molecules, supermolecules and molecular devices. *Angew Chem Int Ed Engl* 27:89–112. doi:10.1002/anie.198800891
- Elhouichet H, Daboussi S, Ajlani H, Najar A, Moadhen A, Oueslati M, Tiginyanu IM, Langa S, Föll H (2005) Strong visible emission from porous GaPdoped with Eu and Tb ions. *J Lumin* 113:329–337. doi:10.1016/j.jlumin.2004.11.003
- Monteiro T, Soares MJ, Neves AJ, Carmo MC, Peres M, Cruz A, Alves E, Wahl U, Rita E, Munoz-SanJose V, Zuniga-Perez J (2006) Luminescence and structural properties of defects in ion implanted ZnO. *Phys Stat Sol C* 3:968–971. doi:10.1002/pssc.200564640
- Chi B, Victorio E-S, Jin T (2006) Synthesis of Eu-doped photoluminescent titania nanotubes via a two-step hydrothermal treatment. *Nanotechnology* 17:2234–2241. doi:10.1088/0957-4484/17/9/027
- Lin K-M, Lin C-C, Li Y-Y (2006) Luminescent properties and characterization of  $\text{Gd}_2\text{O}_3:\text{Eu}^{3+}$ @ $\text{SiO}_2$  and  $\text{Gd}_2\text{Ti}_2\text{O}_7:\text{Eu}^{3+}$ @ $\text{SiO}_2$  core-shell phosphors prepared by a sol–gel process. *Nanotechnology* 17:1745–1751. doi:10.1088/0957-4484/17/6/034
- Serra OA, Nassar EJ, Zapparoli G, Rosa ILV (1994) Organic complexes of  $\text{Eu}^{3+}$  supported in functionalized silica gel: highly luminescent material. *J Alloy Comp* 207–208:454–456. doi:10.1016/0925-8388(94)90262-3
- Serra OA, Nassar EJ, Rosa ILV (1997)  $\text{Tb}^{3+}$  molecular photonic devices supported on silica gel and functionalized silica gel. *J Lumin* 72–74:263–265. doi:10.1016/S0022-2313(96)00391-2
- Xu L, Ma Y-F, Tang K-Z, Tang Y, Liu W-S, Tan M-Y (2008) Preparation, characterization and photophysical properties of highly luminescent terbium complexes incorporated into  $\text{SiO}_2$ /polymer hybrid material. *J Fluoresc* 18:685–693. doi:10.1007/s10895-008-0344-z
- Zhang HJ, Fu LS, Wang SB, Meng QG, Yang KY, Ni JZ (1999) Luminescence characteristics of europium and terbium complexes with 1, 10-phenanthroline in-situ synthesized in a silica matrix by a two-step sol–gel process. *Mater Lett* 38:260–264. doi:10.1016/S0167-577X(98)00169-4
- Lenaerts P, Ryckebosch E, Driesen K, Deun RV, Nockemann P, Görller-Walrand C, Binnemans K (2005) Study of the luminescence of tris(2-thenoyltrifluoroacetato)lanthanide(III) complexes covalently linked to 1, 10-phenanthroline-functionalized hybrid sol–gel glasses. *J Lumin* 114:77–84. doi:10.1016/j.jlumin.2004.12.001
- Trejo-Valdez M, Jenouvrier P, Langlet M (2004) Luminescence properties of ORMOSIL films doped with terbium complexes. *J Non-Cryst Solids* 345–346:628–633. doi:10.1016/j.jnoncrysol.2004.08.112
- Silva RF, Zaniquelli MED (1999) Aluminium doped zinc oxide films: formation process and optical properties. *J Non-Cryst Solids* 247:248–253. doi:10.1016/S0022-3093(99)00079-4
- Reyes R, Cremona M, Teotonio EES, Brito HF, Malta OL (2004) Voltage color tunable OLED with (Sm, Eu)- $\beta$ -diketonate complex blend. *Chem Phys Lett* 396:54–58. doi:10.1016/j.cplett.2004.07.074

14. Quirino WG, Legnani C, Cremona M, Lima PP, Junior SA, Malta OL (2006) White OLED using  $\beta$ -diketones rare earth binuclear complex as emitting layer. *Thin Solid Films* 494:23–27. doi:10.1016/j.tsf.2005.08.185
15. Santos G, Fonseca JF, Andrade AM, Deichmann V, Akcelrud L, Braga SS, Coelho AC, Gonçalves IS, Peres M, Simões W, Monteiro T, Pereira L (2008) Organic light emitting diodes with europium (III) emissive layers based on  $\beta$ -diketonate complexes: the influence of the central ligand. *J Non-Cryst Solids* 354:2897–2900. doi:10.1016/j.jnoncrsol.2007.10.097
16. You H, Ma D (2008) Efficient white organic light-emitting diodes using europium complex as the red unit. *J Phys D Appl Phys* 41. doi:10.1088/0022-3727/41/15/155113
17. Bahnemann DW, Kormann C, Hoffmann MR (1987) Preparation and characterization of quantum size zinc oxide: a detailed spectroscopic study. *J Phys Chem* 91:3789–3798. doi:10.1021/j100298a015
18. Spanhel L, Anderson MA (1991) Semiconductor clusters in the sol–gel process: quantized aggregation, gelation, and crystal growth in concentrated ZnO colloids. *J Am Chem Soc* 113:2826–2833. doi:10.1021/ja00008a004
19. Tang W, Cameron DC (1994) Aluminum-doped zinc oxide transparent conductors deposited by the sol–gel process. *Thin Solid Films* 238:83–87. doi:10.1016/0040-6090(94)90653-X
20. Silva RF, Zaniquelli MED (2004) Aluminium-doped zinc oxide films prepared by an inorganic sol–gel route. *Thin Solid Films* 449:86–93. doi:10.1016/S0040-6090(03)01405-6
21. Che P, Meng J, Guo L (2007) Oriented growth and luminescence of ZnO:Eu films prepared by sol–gel process. *J Lumin* 122:168–171. doi:10.1016/j.jlumin.2006.01.076
22. Liu Z, Li Y (2008) Sol–gel synthesis and luminescence property of ZnO:(La, Eu)Cl nanocomposite thin films. *Thin Solid Films* 516:5557–5561. doi:10.1016/j.tsf.2007.07.122
23. Bünzli J-CG, Choppin GR (1989) *Lanthanide probes in life, chemical and earth science*. Elsevier, Amsterdam, p 238
24. Calefi PS, Ribeiro OA, Pires AM, Serra OA (2002) Characterization and spectroscopic studies of Eu<sup>3+</sup> and Tb<sup>3+</sup> complexes with 2, 2'-bipyridine-4, 4'-dicarboxylic acid. *J Alloy Comp* 344:285–288. doi:10.1016/S0925-8388(02)00370-5
25. Hasegawa Y, Kawai H, Nakamura K, Yasuda N, Wada Y, Yanagida S (2006) Molecular design of luminescent Eu(III) complexes as lanthanide lasing material and their optical properties. *J Alloy Comp* 408–412:669–674. doi:10.1016/j.jallcom.2004.12.145
26. Charles RG, Ohlmann RC (1965) Europium thenoyltrifluoroacetate, preparation and fluorescence properties. *J Inorg Nucl Chem* 27:255–259. doi:10.1016/0022-1902(65)80222-6
27. Malta OL, Brito HF, Menezes JFS, Gonçalves e Silva FR, Alves S Jr, Farias FS Jr, deAndrade AVM (1997) Spectroscopic properties of a new light-converting device Eu(thenoyltrifluoroacetate) 2 (dibenzyl sulfoxide). A theoretical analysis based on structural data obtained from a sparkle model. *J Lumin* 75:255–268
28. Santa-Cruz PA, Teles FS (2003) *Spectra Lux Software v.2.0*. Ponto Quântico Nanodispositivos
29. Wang Z, Liang H, Gong M, Su Q (2007) Luminescence investigation of Eu<sup>3+</sup> activated double molybdates red phosphors with scheelite structure. *J Alloy Comp* 432:308–312. doi:10.1016/j.jallcom.2006.06.008
30. Zhou L, Choy WCH, Shi J, Gong M, Liang H (2006) A novel green emitting phosphor Ca<sub>1.5</sub>Y<sub>1.5</sub>Al<sub>3.5</sub>Si<sub>1.5</sub>O<sub>12</sub>:Tb<sup>3+</sup>. *Mater Chem Phys* 100:372–374. doi:10.1016/j.matchemphys.2006.01.007